

## Plasma Chemistry

International Edition: DOI: 10.1002/anie.201707131  
German Edition: DOI: 10.1002/ange.201707131One-Step Reforming of CO<sub>2</sub> and CH<sub>4</sub> into High-Value Liquid Chemicals and Fuels at Room Temperature by Plasma-Driven Catalysis

Li Wang, Yanhui Yi, Chunfei Wu, Hongchen Guo, and Xin Tu\*

**Abstract:** The conversion of CO<sub>2</sub> with CH<sub>4</sub> into liquid fuels and chemicals in a single-step catalytic process that bypasses the production of syngas remains a challenge. In this study, liquid fuels and chemicals (e.g., acetic acid, methanol, ethanol, and formaldehyde) were synthesized in a one-step process from CO<sub>2</sub> and CH<sub>4</sub> at room temperature (30 °C) and atmospheric pressure for the first time by using a novel plasma reactor with a water electrode. The total selectivity to oxygenates was approximately 50–60%, with acetic acid being the major component at 40.2% selectivity, the highest value reported for acetic acid thus far. Interestingly, the direct plasma synthesis of acetic acid from CH<sub>4</sub> and CO<sub>2</sub> is an ideal reaction with 100% atom economy, but it is almost impossible by thermal catalysis owing to the significant thermodynamic barrier. The combination of plasma and catalyst in this process shows great potential for manipulating the distribution of liquid chemical products in a given process.

Chemical transformations of CO<sub>2</sub> into value-added chemicals and fuels have been regarded as a key element for creating a sustainable low-carbon economy in the chemical and energy industry. A particularly significant route that is currently being developed for CO<sub>2</sub> utilization is catalytic CO<sub>2</sub> hydrogenation. This process can produce a range of fuels and chemicals, including CO, formic acid, methanol, hydrocarbons, and alcohols; however, high H<sub>2</sub> consumptions (CO<sub>2</sub> + 3H<sub>2</sub> → CH<sub>3</sub>OH + H<sub>2</sub>O) and high operating pressures (ca. 30–300 bar) are major challenges associated with this process.

Instead of using H<sub>2</sub>, the direct conversion of CO<sub>2</sub> with CH<sub>4</sub> (dry reforming of methane, DRM) into liquid fuels and chemicals (e.g., acetic acid) represents another promising route for both CO<sub>2</sub> valorization and CH<sub>4</sub> activation. CH<sub>4</sub> is an ideal H supplier to replace H<sub>2</sub> in CO<sub>2</sub> hydrogenation as CH<sub>4</sub> has a high H density and is available from a range of sources (e.g., natural gas, shale gas, biogas, and flared gas). Moreover, it is an inexpensive carbon source that can increase the atom utilization of CO<sub>2</sub> hydrogenation owing to the stoichiometric ratio of C and O atoms, as well as reduce the formation of water.

Recently, Ge and co-workers investigated the direct C–C coupling of CO<sub>2</sub> and CH<sub>4</sub> to form acetic acid on a Zn-doped ceria catalyst by density functional theory (DFT) modeling;<sup>[1]</sup> this is an attractive route as the direct conversion of CO<sub>2</sub> and CH<sub>4</sub> into acetic acid is a reaction with 100% atom economy [Equation (1)]. However, this reaction is thermodynamically



unfavorable under practical conditions. The conventional indirect catalytic process often proceeds through two steps (Scheme 1): 1) DRM to produce syngas (CO and H<sub>2</sub>) at high temperatures (> 700 °C), and 2) conversion of syngas into liquid fuels and chemicals at high pressures. This indirect route for CO<sub>2</sub> valorization and CH<sub>4</sub> activation is inefficient as the DRM process for syngas production is highly endothermic and requires high temperatures and energy input [Equation (2)]. Catalyst deactivation due to carbon deposition is



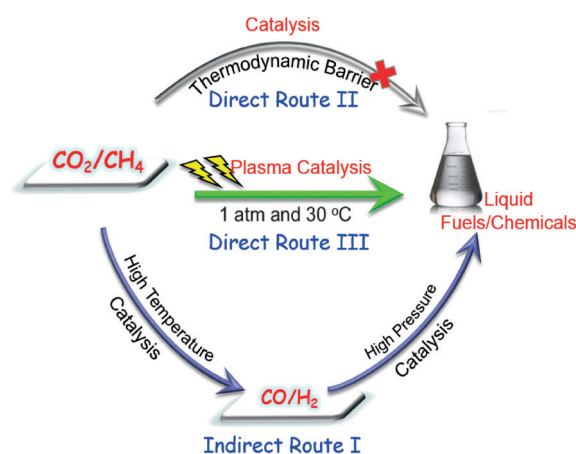
[\*] Dr. L. Wang, Dr. X. Tu  
Department of Electrical Engineering and Electronics  
University of Liverpool  
Liverpool, L69 3GJ (UK)  
E-mail: xin.tu@liv.ac.uk

Dr. Y. Yi, Prof. H. Guo  
State Key Laboratory of Fine Chemicals  
School of Chemical Engineering, Dalian University of Technology  
Dalian, 116024 (P. R. China)

Dr. C. Wu  
School of Engineering, University of Hull  
Hull, HU6 7RX (UK)

Supporting information and the ORCID identification number(s) for the author(s) of this article can be found under:  
<https://doi.org/10.1002/anie.201707131>.

© 2017 The Authors. Published by Wiley-VCH Verlag GmbH & Co. KGaA. This is an open access article under the terms of the Creative Commons Attribution License, which permits use, distribution and reproduction in any medium, provided the original work is properly cited.



**Scheme 1.** Direct and indirect processes for the conversion of CO<sub>2</sub> and CH<sub>4</sub> into liquid fuels and chemicals.

another challenge impacting the use of this reaction on a commercial scale. It is almost impossible to directly convert two stable and inert molecules ( $\text{CO}_2$  and  $\text{CH}_4$ ) into liquid fuels or chemicals in a one-step catalytic process bypassing the production of syngas. A stepwise method was proposed to convert  $\text{CO}_2$  and  $\text{CH}_4$  into acetic acid over Cu/Co-based catalysts,<sup>[2]</sup> Pd/C, Pt/ $\text{Al}_2\text{O}_3$ ,<sup>[3]</sup> Pd/ $\text{SiO}_2$ , and Rh/ $\text{SiO}_2$ <sup>[4]</sup> by heterogeneous catalysis. The catalyst was first exposed to  $\text{CH}_4$ , forming  $\text{CH}_x$  species on the catalyst surface. Subsequently, the feed gas was changed from  $\text{CH}_4$  to  $\text{CO}_2$ , and acetic acid was formed through the reaction of  $\text{CO}_2$  with  $\text{CH}_x$  over the catalyst. This indirect process is complicated by the periodic change of reactants and the product collection.<sup>[5]</sup>

Non-thermal plasmas (NTPs) offer a unique way to enable thermodynamically unfavorable chemical reactions at low temperatures owing to the non-equilibrium character. The overall gas temperature in an NTP remains low while the generated electrons are highly energetic with a typical electron temperature of 1–10 eV, which is sufficient to activate inert molecules (e.g.,  $\text{CO}_2$  and  $\text{CH}_4$ ) into reactive species, including radicals, excited atoms, molecules, and ions. These energetic species are capable of initiating a variety of chemical reactions. Although much effort has been devoted to the use of NTPs for the degradation of gas pollutants, far less has been done with regard to their use in the synthesis of fuels and chemicals.<sup>[6]</sup> Previous work on DRM with NTPs mainly focused on syngas production,<sup>[7]</sup> while very limited efforts have been devoted to the challenging one-step conversion of  $\text{CH}_4$  and  $\text{CO}_2$  into liquid fuels and chemicals.<sup>[8,9]</sup> A few groups have reported on the formation of trace oxygenates (e.g., alcohols and acids) as side products in plasma DRM for syngas production.<sup>[10]</sup> Thus far, the use of NTPs for the direct conversion of  $\text{CO}_2$  and  $\text{CH}_4$  into oxygenates has resulted in poor selectivities and yields.

Herein, we describe the development of a novel dielectric barrier discharge (DBD) reactor with a ground water electrode (see the Supporting Information, Schemes S1 and S2) for the one-step conversion of  $\text{CO}_2$  and  $\text{CH}_4$  into oxygenates at room temperature ( $30^\circ\text{C}$ ) and atmospheric pressure. This setup is unique and has not been reported previously. Figure 1 shows that no reaction occurred in the “catalyst only” mode at  $30^\circ\text{C}$  without plasma. However, the use of an NTP enabled this thermodynamically unfavorable reaction to occur at room temperature and resulted in the production of liquid chemicals, including acetic acid, methanol, ethanol, and acetone, with acetic acid being the major product. Trace amounts of formic acid, propanol, and butanol were also detected in the condensed liquid. In the plasma process without a catalyst (“plasma only”), a total liquid selectivity of 59.1% was achieved with selectivities of 33.7%, 11.9%, 11.9%, and 1.6% for acetic acid, ethanol, methanol, and acetone, respectively (Figure 1a). The CO selectivity was only about 20.0% (Figure 1b), and the  $\text{CH}_4$  and  $\text{CO}_2$  conversions amounted to approximately 18.3% and 15.4%, respectively (Figure 1c).

Combining the plasma process with a catalyst shows great potential for manipulating the production of different oxygenates under ambient conditions. Clearly, packing the Cu/ $\gamma\text{-Al}_2\text{O}_3$  catalyst in the DBD enhanced the selectivity for acetic

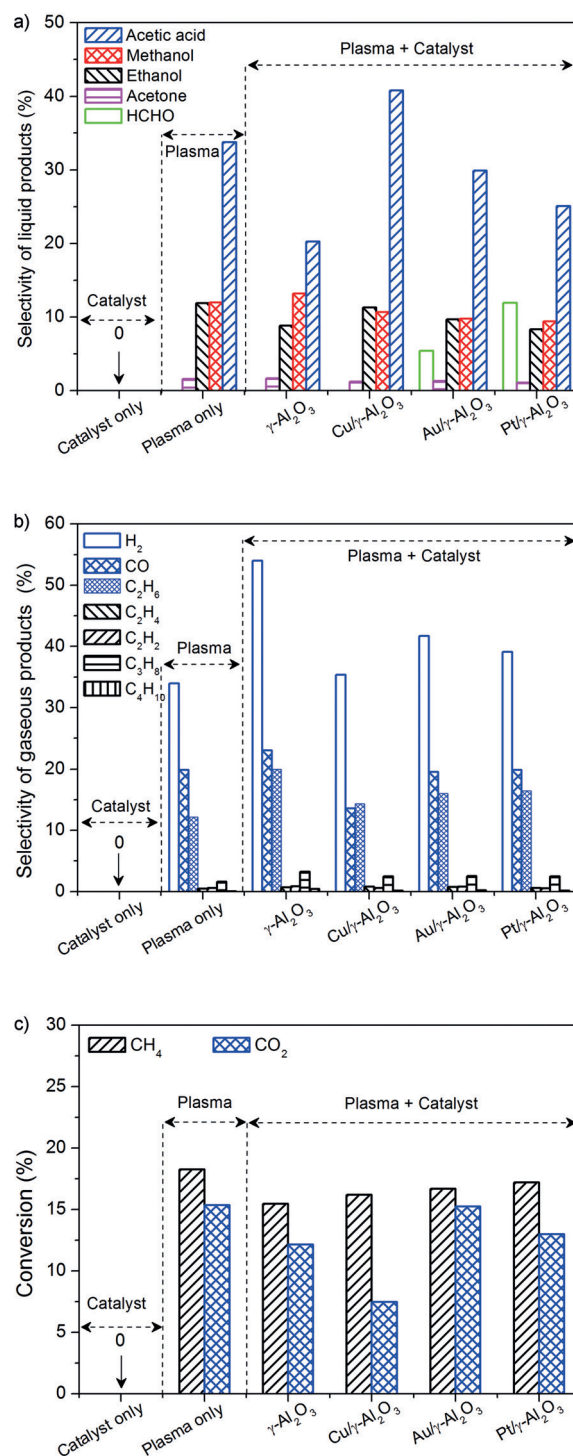


**Figure 1.** Effect of operating modes and catalysts on the reaction: a) Selectivities for oxygenates, b) selectivities for gaseous products, c) conversion of  $\text{CH}_4$  and  $\text{CO}_2$  (total flow rate  $40\text{ mL min}^{-1}$ , discharge power 10 W, catalyst ca. 2 g).

acid to 40.2%, compared to the plasma-only mode and the plasma reaction using  $\gamma\text{-Al}_2\text{O}_3$  only (20.2%). Acetic acid was the major product regardless of the catalyst used, followed by methanol and ethanol (Figure 1a). HCHO was formed only when the supported noble metal catalysts were used in the

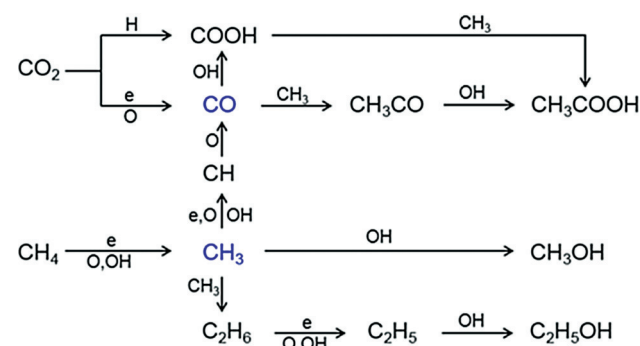
plasma reaction, and the Pt/ $\gamma$ -Al<sub>2</sub>O<sub>3</sub> catalyst showed the highest selectivity to HCHO. Compared to the plasma-only mode, placing the catalysts in the DBD gave similar gaseous product distributions, with H<sub>2</sub>, CO, and C<sub>2</sub>H<sub>6</sub> being the major gaseous products (Figure 1 b). However, combining the NTP with the catalysts enhanced the H<sub>2</sub> selectivity by 10–20% (except for Cu/ $\gamma$ -Al<sub>2</sub>O<sub>3</sub>), and slightly increased C<sub>2</sub>H<sub>6</sub> production, but had a weak effect on the selectivity for CO (except for Cu/ $\gamma$ -Al<sub>2</sub>O<sub>3</sub>, which decreased CO selectivity to 13.5%) and other C<sub>x</sub>H<sub>y</sub> (i.e., C<sub>2</sub>H<sub>2</sub>, C<sub>2</sub>H<sub>4</sub>, C<sub>2</sub>H<sub>6</sub>, C<sub>3</sub>H<sub>8</sub>, and *n*-C<sub>4</sub>H<sub>10</sub>). In addition, compared to the plasma-only mode, the conversion of CO<sub>2</sub> and CH<sub>4</sub> slightly decreased with packing catalysts. This phenomenon can be attributed to the change in discharge behavior induced by the catalyst, which had a negative effect on the reaction (Figure S1). Interestingly, C<sub>6</sub>H<sub>12</sub>O<sub>4</sub> (CAS No. 49653-17-0) was found on the inner reactor wall in the plasma-catalyst mode (Figure S2). These results demonstrate the feasibility of using NTPs for the direct conversion of CH<sub>4</sub> and CO<sub>2</sub> into higher-value liquid fuels and chemicals in a single-step process under ambient conditions, bypassing the formation of syngas.

To understand the formation of the liquid chemicals, optical emission spectroscopy (OES) was used to investigate the species produced in the CH<sub>4</sub>/CO<sub>2</sub> DBD (Figure 2). H <sub>$\alpha$</sub>  and O atomic lines and CH, C<sub>2</sub>, CO<sub>2</sub><sup>+</sup>, CO<sub>2</sub>, and CO bands were identified in the emission spectra of the DBD, with CO, CH, and H being the major ones (Table S2).

CO is mainly derived from reactions S1–S3 (Table S3) in the DBD. Our simulation showed that electron-impact CO<sub>2</sub> reactions produced about 95% vibrationally excited CO<sub>2</sub> (CO<sub>2</sub>(v)) compared to electronically excited CO<sub>2</sub> as shown in Figure S3 and Table S4. O radicals generated from CO<sub>2</sub> dissociation can attack CO<sub>2</sub>(v) molecules to produce CO (S1 and S2).<sup>[11]</sup> Different from CH, CH<sub>3</sub> derived from CH<sub>4</sub> dissociation cannot be detected by OES, but recent simulations revealed that electron-impact dissociation of CH<sub>4</sub> leads to 79% CH<sub>3</sub> formation and only 15% and 5% CH<sub>2</sub> and CH, respectively.<sup>[12]</sup> Therefore, CH<sub>3</sub> is the dominant species in the CH<sub>4</sub>/CO<sub>2</sub> DBD. In addition to electrons (S4 in Table S3),

reactive species such as OH, O, and H can also react with CH<sub>4</sub> to produce CH<sub>3</sub> radicals (S5–S7) in the CH<sub>4</sub>/CO<sub>2</sub> DBD. Additionally, OH is an important species, especially for alcohol formation. In the CH<sub>4</sub>/CO<sub>2</sub> DBD, OH could be produced indirectly by reactions S8–S13, with S8 and S9 as the major channels based on the reaction rate coefficients and *E<sub>a</sub>*.<sup>[13]</sup> Special attention was given to S10, although a very low reaction rate coefficient of  $1.4 \times 10^{-29}$  cm<sup>3</sup> molecule<sup>-1</sup> s<sup>-1</sup> and a high *E<sub>a</sub>* value of 111 kJ mol<sup>-1</sup> were determined for ground-state CO<sub>2</sub> reacting with an H radical to produce an OH radical; this reaction (S10) can be accelerated by using CO<sub>2</sub>(v) instead of ground-state CO<sub>2</sub>.<sup>[14]</sup> and the use of vibrationally excited reagents is most effective in overcoming the activation barrier of the endothermic reaction.<sup>[14,15]</sup> Thus the reaction CO<sub>2</sub>(v) + H → CO + OH could be one of the major routes for OH formation under these conditions as CO<sub>2</sub> is mainly present in vibrationally excited states (Figure S3).

Based on the analysis of the gaseous and condensed liquid products and the OES results, CO, CH<sub>3</sub>, and OH radicals are the key species in the CH<sub>4</sub>/CO<sub>2</sub> plasma reaction. Therefore, possible reaction pathways for the formation of acetic acid, methanol, and ethanol under these conditions are proposed in Scheme 2.



**Scheme 2.** Possible reaction pathways for the formation of CH<sub>3</sub>COOH, CH<sub>3</sub>OH, and C<sub>2</sub>H<sub>5</sub>OH in the direct reforming of CH<sub>4</sub> and CO<sub>2</sub> with DBD.

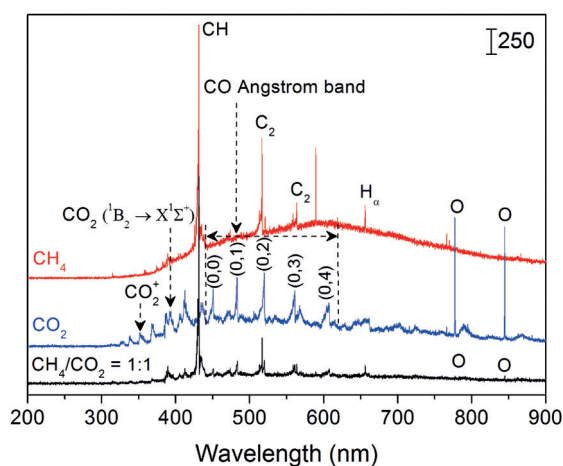


**Figure 2.** Optical emission spectra of CH<sub>4</sub>, CO<sub>2</sub>, and CH<sub>4</sub>/CO<sub>2</sub> plasmas (total flow rate 40 mL min<sup>-1</sup>, CH<sub>4</sub>/CO<sub>2</sub> ratio 1:1, discharge power 10 W, exposure time 2 s).

Two possible reaction pathways could contribute to the formation of acetic acid. CO can react with a CH<sub>3</sub> radical to form an acetyl radical (CH<sub>3</sub>CO) by reaction S14 in Table S3 with a low energy barrier of 28.77 kJ mol<sup>-1</sup>,<sup>[16]</sup> followed by recombination with OH to produce acetic acid in reaction S15 with no energy barrier<sup>[10g]</sup> (see also Figures 3 and S4). Clearly, the selectivity to acetic acid increases initially and then decreases with the CH<sub>4</sub>/CO<sub>2</sub> ratio, with optimal acetic acid formation at a CH<sub>4</sub>/CO<sub>2</sub> ratio of 1:1. Correspondingly, the relative intensities of the CO band head and the O atomic line increased with a decrease in the CH<sub>4</sub>/CO<sub>2</sub> ratio from 3:1 to 1:2 while that of the CH band head increased (Figure S4). This suggests that decreasing the CH<sub>4</sub>/CO<sub>2</sub> molar ratio decreases the generation of CH<sub>3</sub> radicals, but increases OH formation. A similar mechanism of acetic acid formation has been proposed on the basis of DFT modeling<sup>[10g]</sup> and by Eliasson and co-workers.<sup>[10i]</sup> In addition, direct coupling of CH<sub>3</sub> and carboxyl radicals (COOH) could also form acetic acid by

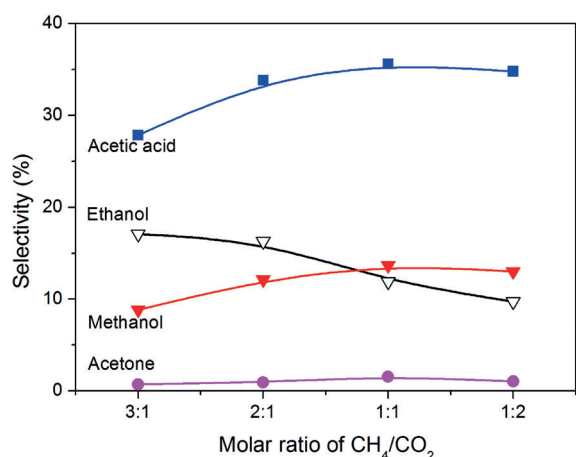


**Figure 3.** Effect of the CH<sub>4</sub>/CO<sub>2</sub> molar ratio on the selectivity for oxygenates without a catalyst (total flow rate 40 mL min<sup>-1</sup>, discharge power 10 W).

reaction S16, while COOH radicals may be formed from reactions S17 and S18 in Table S3.<sup>[10g]</sup>

Decreasing the CH<sub>4</sub>/CO<sub>2</sub> molar ratio decreased the generation of CH<sub>3</sub> radicals, but increased OH formation (Figure S4). Simultaneously, the formation of CH<sub>3</sub>OH increased initially with a decrease in the CH<sub>4</sub>/CO<sub>2</sub> molar ratio and reached a peak at a CH<sub>4</sub>/CO<sub>2</sub> molar ratio of 1:1. By contrast, the formation of C<sub>2</sub>H<sub>5</sub>OH decreased continuously as the CH<sub>4</sub>/CO<sub>2</sub> molar ratio was decreased (Figure 3). These findings suggest that the production of CH<sub>3</sub>OH mainly depends on the generation of both CH<sub>3</sub> and OH radicals while the formation of C<sub>2</sub>H<sub>5</sub>OH is more sensitive to the presence of CH<sub>3</sub> radicals in the plasma reaction as C<sub>2</sub>H<sub>5</sub>OH formation requires twice the amount of CH<sub>3</sub> radicals in comparison to the formation of CH<sub>3</sub>OH. As shown in Scheme 2, CH<sub>3</sub>OH can be directly formed from the coupling of CH<sub>3</sub> and OH radicals with a high rate coefficient (S19 in Table S3),<sup>[17]</sup> while C<sub>2</sub>H<sub>5</sub>OH formation requires several elementary reactions (S20–S24). The recombination of a CH<sub>3</sub> radical with itself forms C<sub>2</sub>H<sub>6</sub> (S20),<sup>[18]</sup> which is followed by dehydrogenation to form a C<sub>2</sub>H<sub>5</sub> radical by reactions S21–S23, with S21 as the primary reaction according to the reaction rates.<sup>[13d,19]</sup> The C<sub>2</sub>H<sub>5</sub> radical finally recombines with OH to form C<sub>2</sub>H<sub>5</sub>OH with a high rate coefficient of 9.34 × 10<sup>-11</sup> cm<sup>3</sup> molecule<sup>-1</sup> s<sup>-1</sup> (S24).<sup>[20]</sup>

Clearly, adding catalysts to the plasma reaction influences the distribution of the formed oxygenates, especially for the formation of HCHO after addition of the Pt and Au catalysts, revealing the occurrence of surface reactions in addition to plasma gas phase reactions.<sup>[21]</sup> In traditional catalysis, CO hydrogenation, CH<sub>3</sub>OH oxidation, and methylene (CH<sub>2</sub>) oxidation can lead to the generation of HCHO over noble-metal catalysts.<sup>[22]</sup> In this plasma process, adding noble-metal catalysts in the plasma had almost no influence on the CO selectivity, but decreased the selectivity for CH<sub>3</sub>OH, C<sub>2</sub>H<sub>5</sub>OH, and CH<sub>3</sub>COOH and increased the selectivity for HCHO and C<sub>2</sub>H<sub>6</sub> (Figure 1a). Considering the major species that are present in the CH<sub>4</sub>/CO<sub>2</sub> DBD, CH<sub>x</sub> (x = 4, 3, and 2) could be the primary source for HCHO formation by

oxidation reactions. Namely, CH<sub>x</sub> in the gas phase could be adsorbed onto the surface of the catalyst to form HCHO by the oxidation of CH<sub>2,ad</sub> (CH<sub>x,ad</sub> + O, H, OH → CH<sub>2,ad</sub>) and to produce C<sub>2</sub>H<sub>6</sub> by self-recombination of CH<sub>3</sub> radicals instead of converting CH<sub>3</sub> into CH<sub>3</sub>OH, C<sub>2</sub>H<sub>5</sub>OH, and CH<sub>3</sub>COOH. This could explain why the presence of the Au and Pt catalysts in the plasma decreased the formation of CH<sub>3</sub>OH, C<sub>2</sub>H<sub>5</sub>OH, and CH<sub>3</sub>COOH, but enhanced the production of C<sub>2</sub>H<sub>6</sub> and HCHO (Figures 1a and b). Possible pathways for the formation of the major oxygenates on the catalyst surface are proposed in Scheme S3. In addition, catalyst characterization (Figures S5–S8) suggested that the metal particle size and interactions between metal and support are not determining factors for the reaction performance (Figure 1), whereas the strength of the bonding of adsorbed intermediates to the catalyst surface, that is, the oxygen adsorption energy (ΔE<sub>O</sub>), could be a good activity descriptor towards the formation of different products in DRM.<sup>[23]</sup>

In conclusion, the one-step room-temperature synthesis of liquid fuels and chemicals from the direct reforming of CO<sub>2</sub> with CH<sub>4</sub> has been achieved by using a novel atmospheric-pressure DBD reactor. The total selectivity for liquid chemicals was approximately 50–60%, with acetic acid as the major product. The CH<sub>4</sub>/CO<sub>2</sub> molar ratio and the type of catalyst can be used to manipulate the production of different oxygenates. These results clearly show that non-thermal plasmas can be used to overcome the thermodynamic barrier for the direct transformation of CH<sub>4</sub> and CO<sub>2</sub> into a range of strategically important platform chemicals, especially for the production of acetic acid with 100% atom economy. Additionally, combining the DBD with noble-metal catalysts produced formaldehyde, which cannot be generated in the same plasma reaction without a catalyst. This finding suggests that new research should be directed at designing a catalyst with high selectivity towards a desirable product.

### Acknowledgements

Support of this work by the EPSRC SUPERGEN Hydrogen & Fuel Cell (H2FC) Programme (EP/J016454/1) ECR Project (Ref. EACPR PS5768) is gratefully acknowledged.

### Conflict of interest

The authors declare no conflict of interest.

**Keywords:** carbon dioxide · heterogeneous catalysis · methane · plasma chemistry · reforming

**How to cite:** *Angew. Chem. Int. Ed.* **2017**, *56*, 13679–13683  
*Angew. Chem.* **2017**, *129*, 13867–13871

- [1] Y. Zhao, C. Cui, J. Han, H. Wang, X. Zhu, Q. Ge, *J. Am. Chem. Soc.* **2016**, *138*, 10191–10198.
- [2] W. Huang, K. C. Xie, J. P. Wang, Z. H. Gao, L. H. Yin, Q. M. Zhu, *J. Catal.* **2001**, *201*, 100–104.
- [3] E. M. Wilcox, G. W. Roberts, J. J. Spivey, *Catal. Today* **2003**, *88*, 83–90.

- [4] Y.-H. Ding, W. Huang, Y.-G. Wang, *Fuel Process. Technol.* **2007**, *88*, 319–324.
- [5] a) A. A. Olajire, *J. CO<sub>2</sub> Util.* **2013**, *3–4*, 74–92; b) A. Otto, T. Grube, S. Schiebahn, D. Stolten, *Energy Environ. Sci.* **2015**, *8*, 3283–3297; c) I. Dimitriou, P. García-Gutiérrez, R. H. Elder, R. M. Cuéllar-Franca, A. Azapagic, R. W. Allen, *Energy Environ. Sci.* **2015**, *8*, 1775–1789; d) M.-S. Fan, A. Z. Abdullah, S. Bhatia, *ChemCatChem* **2009**, *1*, 192–208; e) D. Pakhare, J. Spivey, *Chem. Soc. Rev.* **2014**, *43*, 7813–7837; f) V. Havran, M. P. Dudukovic, C. S. Lo, *Ind. Eng. Chem. Res.* **2011**, *50*, 7089–7100.
- [6] C. E. Stere, J. A. Anderson, S. Chansai, J. J. Delgado, A. Goguet, W. G. Graham, C. Hardacre, S. Taylor, X. Tu, Z. Wang, *Angew. Chem. Int. Ed.* **2017**, *56*, 5579–5583; *Angew. Chem.* **2017**, *129*, 5671–5675.
- [7] a) W.-C. Chung, M.-B. Chang, *Renewable Sustainable Energy Rev.* **2016**, *62*, 13–31; b) A. Lebouvier, S. A. Iwarere, P. d'Argenlieu, D. Ramjugernath, L. Fulcheri, *Energy Fuels* **2013**, *27*, 2712–2722; c) X. Tao, M. Bai, X. Li, H. Long, S. Shang, Y. Yin, X. Dai, *Prog. Energy Combust. Sci.* **2011**, *37*, 113–124; d) X. Tu, J. C. Whitehead, *Int. J. Hydrogen Energy* **2014**, *39*, 9658–9669.
- [8] J.-J. Zou, Y.-p. Zhang, C.-J. Liu, Y. Li, B. Eliasson, *Plasma Chem. Plasma Process.* **2003**, *23*, 69–82.
- [9] M. Scapinello, L. M. Martini, P. Tosi, *Plasma Processes Polym.* **2014**, *11*, 624–628.
- [10] a) K. Kozlov, P. Michel, H.-E. Wagner, *Plasmas Polym.* **2000**, *5*, 129–150; b) G. R. Dey, T. N. Das, *Plasma Chem. Plasma Process.* **2006**, *26*, 495–505; c) A. Gómez-Ramírez, V. J. Rico, J. Cotrino, A. R. González-Eliphe, R. M. Lambert, *ACS Catal.* **2014**, *4*, 402–408; d) V. Goujard, J.-M. Tatibouët, C. Batiot-Dupeyrat, *Appl. Catal. A* **2009**, *353*, 228–235; e) J. Sentek, K. Krawczyk, M. Młotek, M. Kalczevska, T. Kroker, T. Kolb, A. Schenk, K.-H. Gericke, K. Schmidt-Szałowski, *Appl. Catal. B* **2010**, *94*, 19–26; f) K. Krawczyk, M. Młotek, B. Ulejczyk, K. Schmidt-Szałowski, *Fuel* **2014**, *117*, 608–617; g) L. M. Martini, G. Dilecce, G. Guella, A. Maranzana, G. Tonachini, P. Tosi, *Chem. Phys. Lett.* **2014**, *593*, 55–60; h) C. Liu, J. Wang, Y. Wang, B. Eliasson, *Fuel Chem. Div. Prepr.* **2003**, *48*, 268; i) J. G. Wang, C. J. Liu, B. Eliasson, *Energy Fuels* **2004**, *18*, 148–153.
- [11] A. Fridman, *Plasma Chemistry*, Cambridge University Press, **2008**.
- [12] C. De Bie, B. Verheyde, T. Martens, J. van Dijk, S. Paulussen, A. Bogaerts, *Plasma Processes Polym.* **2011**, *8*, 1033–1058.
- [13] a) J. Murrell, J. Rodriguez, *J. Mol. Struct. THEOCHEM* **1986**, *139*, 267–276; b) D. C. Robie, S. Arepalli, N. Presser, T. Kitsopoulos, R. J. Gordon, *J. Chem. Phys.* **1990**, *92*, 7382–7393; c) W. Tsang, R. Hampson, *J. Phys. Chem. Ref. Data* **1986**, *15*, 1087–1279; d) D. Baulch, C. Cobos, R. Cox, C. Esser, P. Frank, T. Just, J. Kerr, M. Pilling, J. Troe, R. Walker, *J. Phys. Chem. Ref. Data* **1992**, *21*, 411–734; e) S. P. Karkach, V. I. Osherov, *J. Chem. Phys.* **1999**, *110*, 11918–11927.
- [14] V. Rusanov, A. Fridman, G. Sholin, *Phys. Usp.* **1981**, *24*, 447–474.
- [15] J. C. Polanyi, *Science* **1987**, *236*, 680–690.
- [16] D. Baulch, C. Cobos, R. Cox, P. Frank, G. Hayman, T. Just, J. Kerr, T. Murrells, M. Pilling, J. Troe, *J. Phys. Chem. Ref. Data* **1994**, *23*, 847–848.
- [17] A. W. Jasper, S. J. Klippenstein, L. B. Harding, B. Ruscic, *J. Phys. Chem. A* **2007**, *111*, 3932–3950.
- [18] R. Gomer, G. Kistiakowsky, *J. Chem. Phys.* **1951**, *19*, 85–91.
- [19] R. Atkinson, D. Baulch, R. Cox, R. Hampson, Jr., J. Kerr, M. Rossi, J. Troe, *J. Phys. Chem. Ref. Data* **1997**, *26*, 521–1011.
- [20] R. Sivaramakrishnan, M.-C. Su, J. Michael, S. Klippenstein, L. Harding, B. Ruscic, *J. Phys. Chem. A* **2010**, *114*, 9425–9439.
- [21] L. Wang, Y. Zhao, C. Liu, W. Gong, H. Guo, *Chem. Commun.* **2013**, *49*, 3787–3789.
- [22] a) Z.-Z. Lin, X. Chen, *Mater. Des.* **2016**, *107*, 82–89; b) S. Yin, Z. Wang, E. R. Bernstein, *Phys. Chem. Chem. Phys.* **2013**, *15*, 4699–4706; c) I. Sobczak, M. Kozłowska, M. Ziolek, *J. Mol. Catal. A* **2014**, *390*, 114–124; d) K. Czelej, K. Cwieka, J. C. Colmenares, K. J. Kurzydłowski, *Langmuir* **2016**, *32*, 7493–7502; e) J. Niu, J. Ran, R. Wang, X. Du, *Comput. Theor. Chem.* **2015**, *1067*, 40–47.
- [23] a) S. Kattel, B. Yan, Y. Yang, J. G. Chen, P. Liu, *J. Am. Chem. Soc.* **2016**, *138*, 12440–12450; b) M. Behrens, F. Studt, I. Kasatkin, S. Köhl, M. Hävecker, F. Abild-Pedersen, S. Zander, F. Girgsdies, P. Kurr, B.-L. Kniep, *Science* **2012**, *336*, 893–897; c) F. Studt, I. Sharafutdinov, F. Abild-Pedersen, C. F. Elkjær, J. S. Hummelshøj, S. Dahl, I. Chorkendorff, J. K. Nørskov, *Nat. Chem.* **2014**, *6*, 320–324.

Manuscript received: July 13, 2017

Accepted manuscript online: August 25, 2017

Version of record online: September 19, 2017